Transactions of JWRI, Vol. 34 (2005), No. 1

Effect of Interfacial Reaction Layer on Bond Strength of Friction-Bonded Joint of Al Alloys to Steel†

IKEUCHI Kenji *, YAMAMOTO Naotsugu **, TKAHASHI Makoto *, ARITOSHI Masatoshi ******

Abstract

Joining Al alloy to steel has recently absorbed much attention to meet the requirement for the weight reduction of the transportation from an ecological point of view. As reviewed by Wallach and Elliot in 1981, it has long been accepted that the intermetallic compound (IMC) layer forming at the interface has a critical influence on the joint strength of the Al alloy to steel, and a serious impairment is brought about when its thickness exceeds a few μm. Several recent papers regarding the friction bonding of high-strength Al alloys such as 5000 and 6000 series to steel, however, have reported cases where joints exhibited a premature fracture at the interface on tensile test even when the IMC layer was no more than 1 μm in thickness. In order to reveal metallographic factors controlling the joint strength in these cases, the microstructure of the friction-bonded interface of the high-strength Al alloys to mild steel has been investigated on the basis of close observations with a TEM. It turned out that cracks on tensile test propagated through the IMC layer of 200 nm thickness, suggesting that the IMC layer much thinner than 1 μm was responsible for the brittle fracture in the interfacial region. It was also suggested that minor alloying elements in the Al alloy influenced significantly the kind of IMCs formed at the interface. The nano-scale investigation of the interfacial region will contribute greatly to the enhancement of the performance and reliability of the joint of Al alloy and steel.

KEY WORDS: (Friction Bonding) (Aluminum Alloys) (Steel) (Dissimilar Metals Joint) (Intermetallic Compound) (Oxide Film) (TEM Observation)

1. Introduction

Recently, weight reduction and enhancement of the energy efficiency of vehicles are strongly demanded mainly from an ecological point of view. In order to meet these demands, Al alloys will be used more widely for car body and mechanical parts. However, steels still remain indispensable structural materials because of their mechanical properties and cost. Therefore, reliable and efficient processes for joining Al alloys to steels are required. However, the joining of Al alloy to steel is not easy for following reasons:

(1) much higher melting points of steels than Al alloys,
(2) great difference in thermal expansion coefficients between steel and Al alloy,
(3) very tenacious superficial oxide film of the Al alloy, which interferes with the achievement of metal-to-metal contact at the interface, and
(4) formation of the brittle intermetallic compound (IMC) of the Al-Fe system.

The most serious problem of these may be the formation of brittle intermetallic compounds resulting from the reaction of Al with Fe. In particular, fusion welding involves the formation of large amounts of intermetallic compounds in the weld metal because the steel and Al alloy are mixed in the liquid state. Since 1970, several attempts[1, 2, 3] have been made to apply high energy density heat sources like electron beam and laser beam to fusion-welding dissimilar metals combinations which form intermetallic compounds, but it is still quite difficult to control the formation of intermetallic compounds of Al-Fe system within a few μm in size even by precisely controlling the beam power and incident position (distance from the weld line) [4]. In resistance spot welds of an aluminum sheet to a steel, an intermetallic compound layer of a few μm thickness was also observed, although the welding time was within several seconds [5].

In contrast, the formation of the intermetallic compound in solid-state-bonded joints can be controlled

† Received on July 1, 2005
* Professor
** Graduate Student
*** Assistant Professor
**** Hyogo Prefectural Institute for Industrial Research
Transactions of JWRI is published by Joining and Welding Research Institute, Osaka University, Ibaraki, Osaka 567-0047, Japan

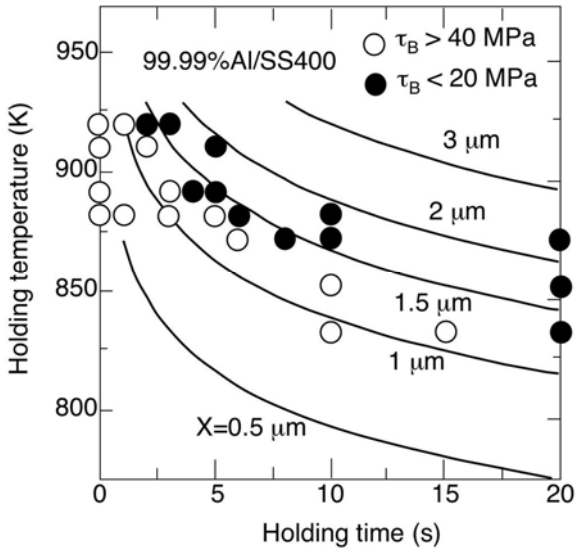

Fig. 1 Effects of heat treatment temperature and time on the thickness of the intermetallic compound layer and shear strength of a roll-bonded joint of a pure aluminum plate to a steel SS400 [9].

by selecting suitable bonding parameters, since the reaction is controlled through the diffusion of reacting elements in the solid state. For this, many investigations have been reported of the solid-state bonding of the Al alloy to the steel. In 1954, Tylecote[6] reported that an aluminum plate could be joined to a steel plate by cold roll bonding when the deformation rate exceeded 40%. In this report, he observed a serious reduction in the joint strength when the joint was held at 873 K for 1.8 ks, and concluded that the intermetallic compound of Al-Fe system was responsible for this degradation.

By reviewing previous reports concerning the solid-state bonding of the Al alloy to the steel, Wallach and Elliot[7, 8] suggested in 1981 that a serious impairment in joint strength is caused by the intermetallic compound (IMC) layer thicker than about 1 μm. They also suggested that the Mg addition to the Al alloy enhances the growth of the IMC layer and so reduces the joint strength, while the Si addition retards the growth of the IMC layer and improves the joint strength. Since then, many papers have been reported about the effect of the IMC layer on the solid-state-bonded joint of Al alloy to steel. The effects of post bonding heat treatments (PBHT) on the thickness of the IMC layer and shear strength of roll-bonded joints of an aluminum plate to a mild steel plate are shown in **Fig. 1**[9]. The thickness of the IMC layer increased with temperature and time of the PBHT, and the shear strength decreased by almost 50% when the IMC layer exceeded 1 – 1.5 μm. On the other hand, **Fig. 2**[10] shows that the IMC layer, no more than ~ 1 μm in thickness, lowers the peel strength considerably, suggesting that the effect of the IMC layer on the joint strength depends on the test method.

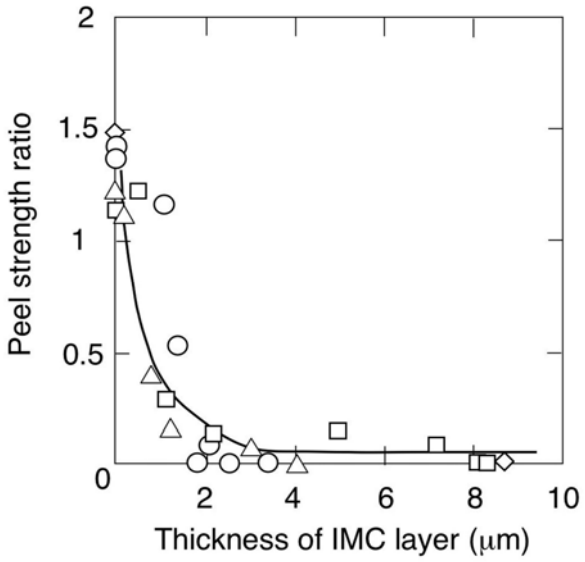

Fig. 2 Relation between peel strength and thickness of IMC layer of roll-bonded joints of aluminum to steel [10].

Friction bonding is a process most widely used for joining of dissimilar metals involving the combination of Al alloy and steel in many industrial fields because of its high productivity and reliability of the joint performance in addition to the controllability of the formation of the IMC layer. However, several authors have reported cases where friction-bonded joints of Al-alloy to steel were fractured at the bond interface showing lower strength than the base metal, even when the IMC layer was less than 1 μm thick[11, 12]. In this regard, no clear explanation has been given for the controlling factor of the joint strength. In particular, Al alloys of high Mg contents showed poorer joint efficiency and narrower bonding parameters ranges to obtain favorable joint efficiency. Therefore, we pursued an investigation of the nano-scale microstructure of friction bonded interfaces of Al alloys to steel, aimed at obtaining a deeper insight into the controlling factors of joint strength of the friction-bonding of Al-Mg alloys to steel and effects of alloying elements of Al-alloys when the IMC layer was less than 1 μm thick.

2. Experimental

Round bars of low carbon steel S10C, commercially pure aluminum A1070, and Al-Mg alloys A5052 and A5083 were employed for the specimen to be bonded. Their chemical compositions are shown in **Tables 1 and 2**. The specimen to be bonded was a round bar of 19 mm diameter with a protrusion of 25 mm length and 16 mm diameter. The end face of the protrusion was the faying surface, which was finished by machining with a lathe to 1.6 μmRa. The friction bonding was carried out with a

Table 1 Chemical composition of the steel S10C employed (mass%).

	C	Si	Mn	Cu	P	S	Ni	Cr	Fe
S10C	0.11	0.16	0.33	0.07	0.01	0.02	0.04	0.08	Bal.

Table 2 Chemical compositions of the Al alloys employed (mass%).

Alloys	Si	Fe	Cu	Mn	Mg	Cr	Zn	Ti	V	Al
A5052	0.11	0.15	0.01	0.02	2.50	0.23	0.01	--	--	Bal.
A5083	0.07	0.11	0.00	0.67	4.40	0.08	0.00	0.01	--	Bal.
A1070	0.08	0.10	0.01	0.00	0.01	0.01	0.00	0.01	0.01	Bal

Table 3 Bonding parameters employed.

Al alloys	Friction pressure, P_1/MPa	Friction time, t_1/s	Forge pressure, P_2/MPa	Forge time, t_2/s	Rotation speed, N/s^{-1}
A5052	20, 40	1 – 5	230	6	20
A5083	40	1 – 4	230	6	20
A1070	20	0.5 – 2	100	6	20

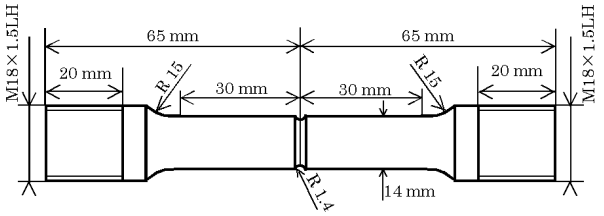

Fig. 3 Dimensions of the specimen for tensile test (in mm).

direct drive machine by pressing an unrotated Al alloy specimen against a rotated low carbon steel specimen. Bonding parameters employed are shown in **Table 3**. The bond strength of the joint interfaces was estimated from tensile strength of a specimen with a circumferential notch at the interface as shown in **Fig. 3**. The tensile test was carried out at room temperatures. The microstructure of the bond interface was investigated mainly by TEM observations. Specimens for TEM observation were cut with a focused ion beam system from a position ~5 mm away from the center axis of the joint. This position was selected because SEM observations at lower magnifications indicated that both IMC layer and fracture morphology of the joint observed at this position occupied almost the whole area of the bond interface.

3. Experimental Results and Discussion

3.1 Friction Bonding of Al-Mg Alloy A5052 to Steel S10C [13)]

Results from the tensile test of the notched specimen of the A5052/S10C joint are shown in **Fig. 4**. The tensile strength was increased with friction time t_1 until t_1 = 4 s, and then decreased with a further increase in t_1. All the tested specimens were fractured near the joint interface. In order to explain these results, the fracture morphology and microstructure of the interface were investigated. When the friction time was 1 s, the fractured surface of the steel side after the tensile test exhibited a quite flat morphology as shown in **Fig. 5**(a). The fractured surface of the steel side and corresponding Al alloy side observed at a higher magnification are shown in **Figs. 5(b) and 5(c)**. Ductile fracture morphologies were observed in a very limited area even at this magnification, and grooves caused by machining with a lathe were observed clearly.

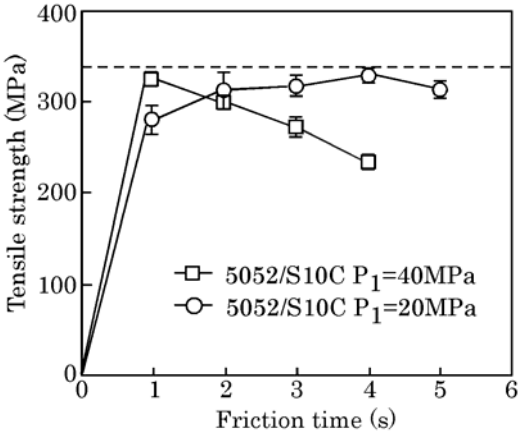

Fig. 4 Tensile strength vs. friction time for the A5052/S10C joint.

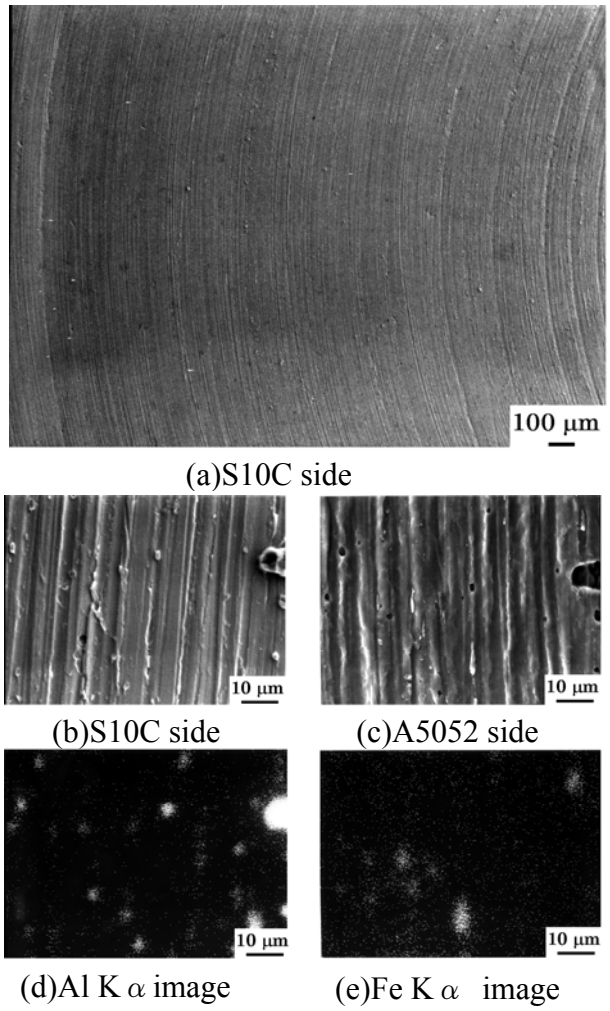

Fig. 5 Fractured surfaces of a A5052/S10C joint (t_1=1 s): (a) fractured surface of the steel side, (b) fractured surface of the steel side observed at a higher magnification, (c) fractured surface conjugate to (b), (d) distribution of Al analyzed by EDX in the area shown in (b), and (e) distribution of Fe analyzed by EDX in the area shown in (c).

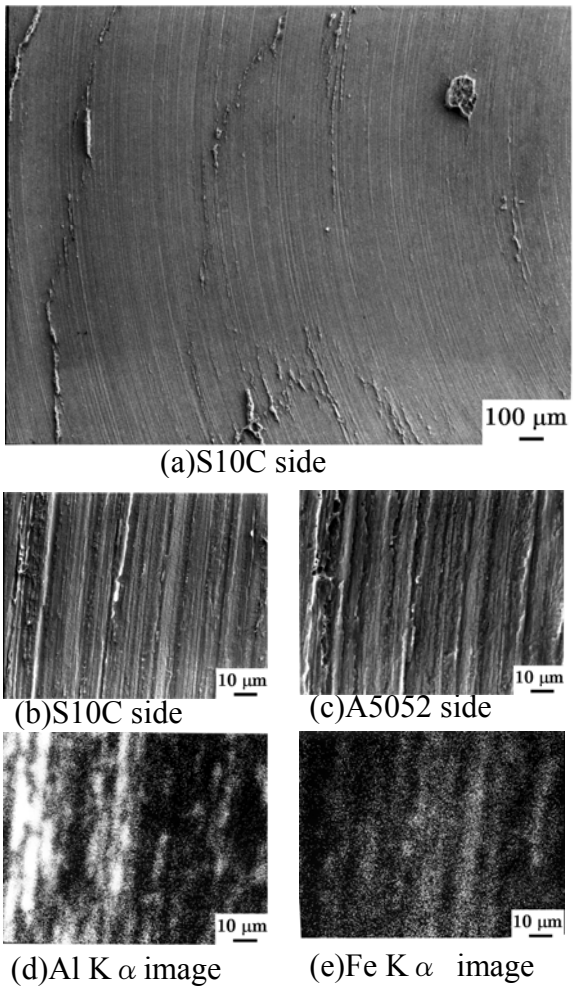

Fig. 6 Fractured surfaces of a A5052/S10C joint (t_1=4 s): (a) fractured surface of the steel side, (b) fractured surface of the steel side observed at a higher magnification, (c) fractured surface conjugate to (b), (d) distribution of Al analyzed by EDX in the area shown in (b), and (e) distribution of Fe analyzed by EDX in the area shown in (c).

EDX analyses of these fractured surfaces detected only small amount of Al on the steel side fractured surface (see **Fig. 5(d)**) and only small amount of Fe on Al alloy side fractured surface (see in **Fig. 5(e)**). This suggests that only small amount of Al-Fe compound was formed at the interface. When the friction time was increased to 4 s, the fracture surface of the joint observed at a low magnification was also quite flat as shown in **Fig. 6(a)**. As shown in **Figs. 6(b) and 6(c)**, however, grooves formed by turning in a lathe had disappeared, and EDX analyses of these fractured surfaces detected considerable amounts of Al on the steel side surface (see **Fig. 6(d)**) and Fe on the Al alloy side (see **Fig. 6(e)**). These results suggest that the joint was fractured in a brittle microstructure consisting of Al and Fe, as the friction time was increased. When the friction time was 5 s, the joint exhibited the fractured morphology similar to those shown in Fig. 6.

In order to reveal the microstructure controlling the tensile strength of the joint, the bond interface was closely observed with a TEM. As shown in **Fig. 7(a)**, an IMC layer ~100 nm thick was observed partially, when the friction time is 1s. From this IMC layer, Fe_2Al_5 was detected based on selected area diffraction (SAD) patterns. Between this IMC layer and the steel substrate, an Al-oxide layer ~10 nm thick was detected by EDX analyses. This oxide layer was observed over almost the whole interface regardless of the presence of the IMC layer. It can be considered that this Al oxide layer was responsible for the flat fracture surface of the joint and fracture strength lower than the base metal. As the friction time was increased, the Al oxide disappeared, and the thickness of the intermetallic compound layer was increased. As is shown in **Fig. 7(b)**, an IMC layer about 400 nm thick was observed continuously between the steel and Al alloy substrates, when the friction time was 4 s. In this IMC layer, Fe_2Al_5, Fe_4Al_{13} and $FeAl_2$ were detected on the basis of SAD patterns. When the friction time was increased to 5 s, the IMC layer consisting of Fe_2Al_5, Fe_4Al_{13} and $FeAl_2$ became about 500 nm thick, as shown in **Fig. 7(c)**. The amount of $FeAl_2$ was much less than those of Fe_2Al_5 and Fe_4Al_{13}. These intermetallic compounds were granular and randomly distributed in the layer. In contrast, each of those observed in the diffusion couple and joint welded by other processes forms layers,

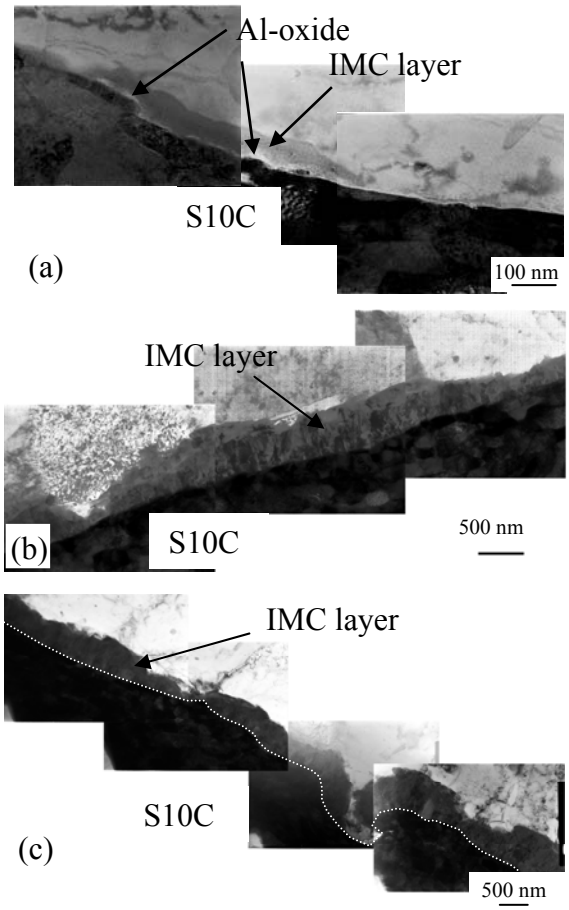

Fig. 7 TEM micrographs of A5052/S10C joints: (a) t_1=1 s, (b) t_1=4 s, and (c) t_1=5 s.

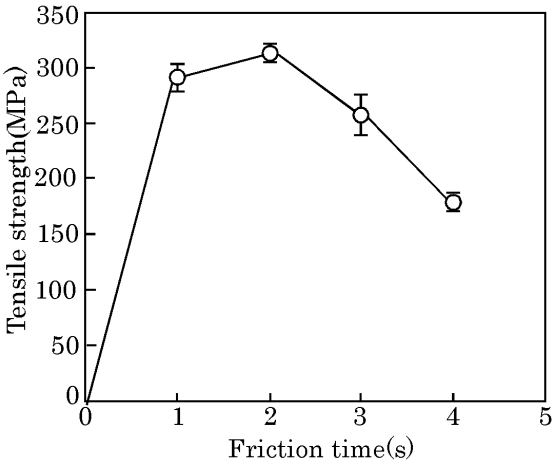

Fig. 8 Tensile strength vs. friction time for the A5083/S10C joint.

which were arranged in the order of their chemical compositions [14]. Therefore, the intermetallic compounds observed in the friction-bonded joint of A5052/S10C can be considered to be formed under the strong influence of a mechanism different from the diffusion of Al and Fe. As suggested by the observations of the fractured surfaces, the A5052/S10C joint was fractured through this IMC layer, when friction time t_1 was 4 s or more.

3.2 Friction Bonding of Al –Mg Alloy A5083 to Steel S10C [15, 16]

The tensile strength of the notched specimen of the A5083/steel joint is plotted against friction time t_1 in **Fig. 8**. The tensile strength rose with increasing friction time t_1 at first, and then lowered, taking a maximum value at t_1 = 2 s. All the tested specimens fractured near the joint interface. When the friction time was shorter than that to obtain the maximum strength, the fracture surface of the joint showed quite flat and featureless morphology, leaving the trace of grooves formed by machining with a lathe as shown in **Fig. 9(a)**. The fractured surfaces of the steel side and corresponding area of the Al alloy side observed at a higher magnification are shown in **Figs. 9(b) and 9(c)**. Ductile fracture morphologies were observed in only limited areas even at this magnification. EDX analyses of these fractured surfaces detected only small amount of Al on the steel side fractured surface (see **Fig. 9(d)**) and small amount of Fe on the Al alloy side (see **Fig. 9(e)**). This suggests that only small amounts of Al-Fe compound were formed at the interface. When the friction time was 2 s at which the maximum strength was obtained, the fractured surface of the joint showed morphology as shown in **Fig. 10**. Even the joint having the maximum strength showed ductile fracture morphologies within only limited areas as shown in **Figs. 10(a) – 10 (c)**. However, the considerable amount of Al was detected on the fractured surface of the steel side by EDX analyses (Fig. 10(d)) and the considerable amount of Fe on the fractured surface of the Al alloy side (**Fig. 10(e)**). These results suggest that this joint having the

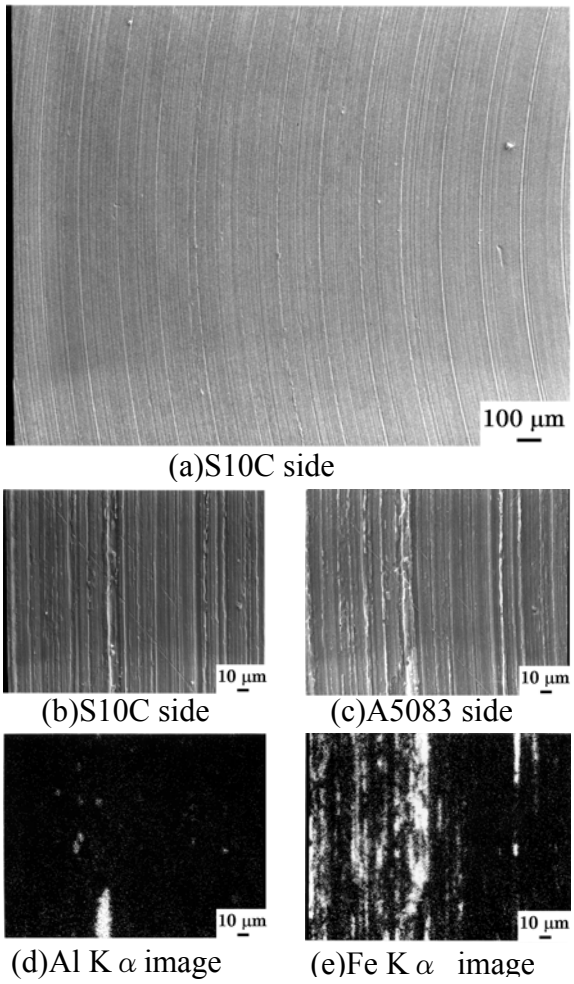

Fig. 9 Fractured surfaces of a A5083/S10C joint (t_1=1 s): (a) fractured surface of the steel side, (b) fractured surface of the steel side observed at a higher magnification, (c) fractured surface conjugate to (b), (d) distribution of Al analyzed by EDX in the area shown in (b), and (e) distribution of Fe analyzed by EDX in the area shown in (c).

maximum strength was fractured in a brittle manner through intermetallic compounds of the Al – Fe system. When t_1 was increased to 3 – 4 s, fractured morphologies of joints were similar to that observed in Fig. 10.

The interfacial microstructures of these joints were closely observed with a TEM[5]. When the friction time was 1 s, a layer about 100 nm thick was detected as shown in **Fig. 11(a)**. Intermetallic compounds involved in this layer were identified as $(Fe,Mn)Al_6$ and Mg_2Si on the basis of SAD patterns. The compounds of $(Fe,Mn)Al_6$ and Mg_2Si were not observed in the joint of A5052 to steel. The formations of these compounds reflect the higher contents of Mn and Mg in the A5083 alloy as shown in Table 2. As can be seen from the ternary phase diagram of Al-Fe-Mn system (see **Fig. 12**) [17], only small addition of Fe to the Al-Mn solid solution causes the precipitation of $MnAl_6$ at Mn contents of 0.2 – 0.7% at 898 K, although no compound of this chemical composition forms in the Al-Fe binary system.

In addition, an Al-oxide film of a thickness less than

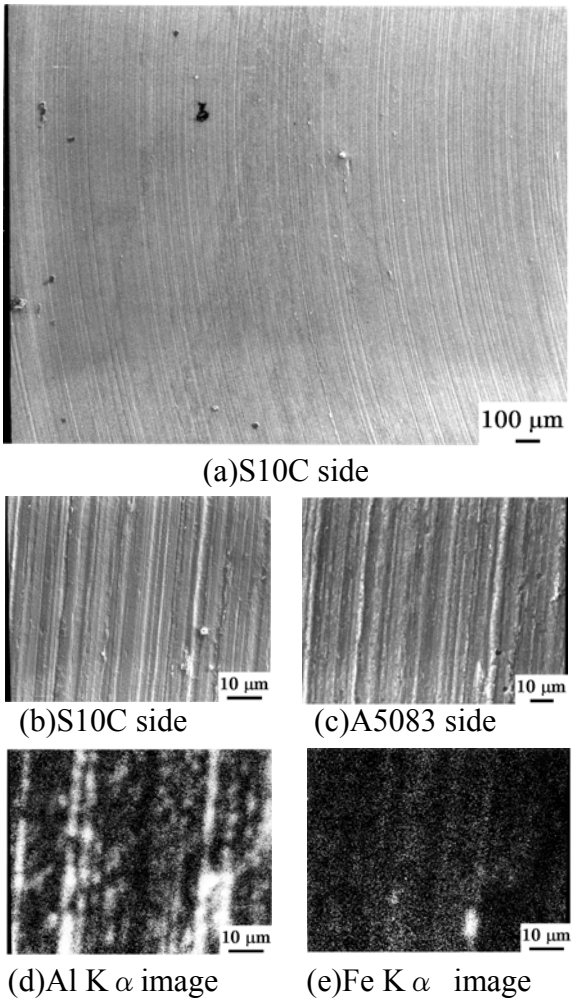

Fig. 10 Fractured surfaces of a A5083/S10C joint (t_1=2 s): (a) fractured surface of the steel side, (b) fractured surface of the steel side observed at a higher magnification, (c) fractured surface conjugate to (b), (d) distribution of Al analyzed by EDX in the area shown in (b), and (e) distribution of Fe analyzed by EDX in the area shown in (c).

10 nm was detected in between the layer of the intermetallic compounds and the steel substrate (see **Fig. 11(a)**) by EDX analyses. Considering the fractured morphology shown in Fig. 9, it can be considered that the joint was fractured mainly at the Al oxide film; i.e., the bond strength of the joint was controlled by the Al-oxide film, when the friction time was 1s.

In a joint showing the maximum bond strength (t_1 = 2 s), no Al-oxide film could be detected between the steel substrate and IMCs layer (see **Fig. 11(b)**). In this IMCs layer, Fe_4Al_{13} and Fe_2Al_5 were detected in addition to $(Fe,Mn)Al_6$, and Mg_2Si by SAD analyses. The thickness of the layer consisting of these intermetallic compounds was increased to about 300 nm. The fracture morphologies and EDX analyses shown in Fig. 10 suggest that the joint was fractured in this IMCs layer when t_1 = 2 s. Thus, the Al oxide film disappeared, as the friction time was increased, and the fracture on the tensile test occurred in the IMCs layer. This means that the

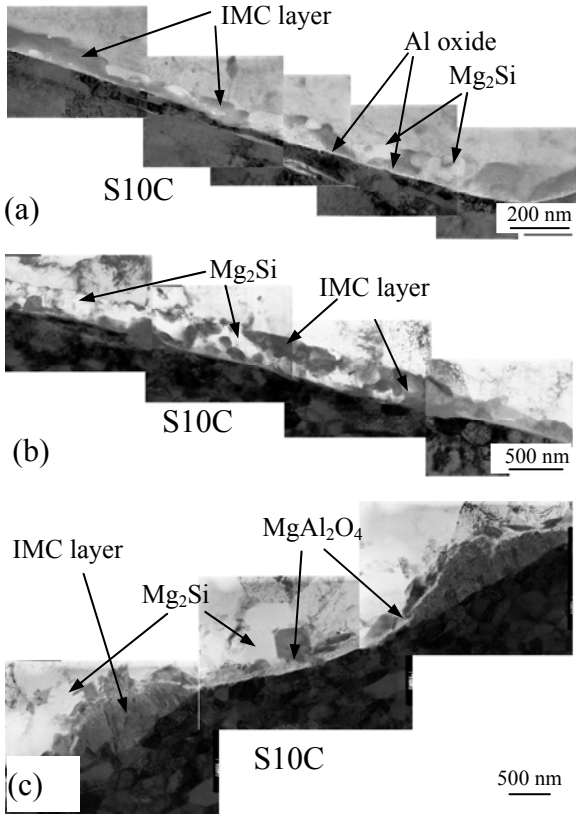

Fig. 11 TEM micrographs of A5083/S10C joints: (a) t_1=1 s, (b) t_1=2 s, and (c) t_1=4 s.

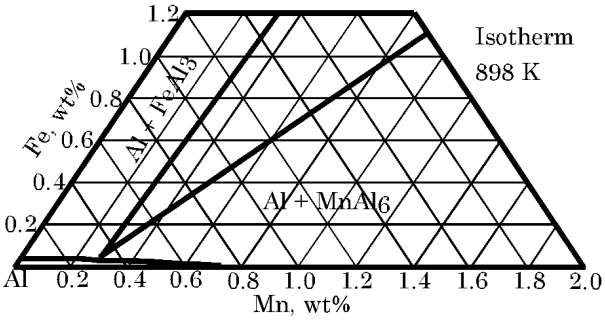

Fig. 12 Ternary phase diagram of the Al-Fe-Mn system.

controlling factor of the bond strength of the A5083/S10C joint was altered from the Al-oxide film to the IMCs layer, as the friction time was increased.

When the friction time was increased to 4 s, the kinds of the intermetallic compounds observed were the same as those observed in the joint having the maximum strength (t_1 = 2 s), and the thickness of the layer of the intermetallic compounds was slightly increased. However, a layer of $MgAl_2O_4$ was observed in addition to the intermetallic compounds (see Fig. 11(c)). The thickness of this layer was about 100 nm. The formation of the $MgAl_2O_4$ layer in the A5083/S10C joint is difficult to explain. As far as we observed with a TEM, no source for oxygen sufficient to form the $MgAl_2O_4$ layer of ~100 nm thickness was found in the base metals or the region

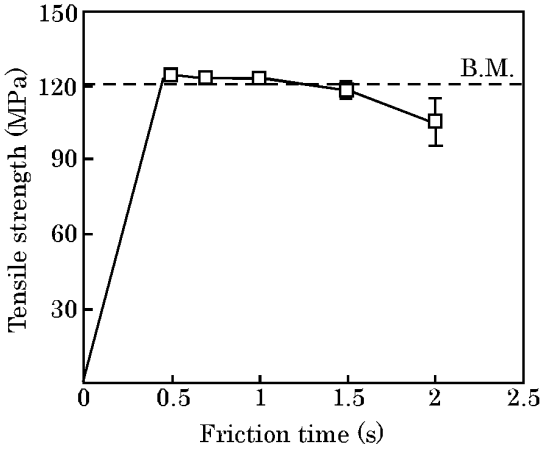

Fig. 13 Tensile strength vs. friction time for the A1070/S10C joint.

around the interface, which suggests that the oxidation of Al and Mg occurred through the reaction with the air during the friction bonding. In this respect, it has been said that the true contact between the faying surfaces is achieved within only limited areas during friction process and in the rest gaps remain between the faying surfaces [18]. Probably, the air was supplied through this gap. It is conceivable that the lower plastic flow rate of the 5083 alloy indicated by the smaller axial displacement during the friction process and higher Mg content than the 5052 alloy contributed to the enhancement of the oxidation of Al and Mg during the friction process. Since the $MgAl_2O_4$ layer was not observed under the other bonding conditions, this oxide layer can be considered to be responsible for the lower strength of this joint than the others (see Fig. 8).

The intermetallic compounds of the Al-Fe system observed in the A5083/S10C joint were granular and randomly distributed in the layer at the interface similar to those observed in the A5052/S10C joint. This suggests that the intermetallic compounds observed in the A5083/S10C joint were formed under the strong influence of a mechanism different from the diffusion of Al and Fe as mentioned in §3.1.

3.3 Friction Bonding of Commercially Pure Aluminum A1070 to Steel S10C [19]

As shown in **Fig. 13**, the tensile strength of the A1070/S10C joint increased rapidly with friction time t_1. The joint showed a maximum tensile strength when t_1 = 0.5 s, and was fractured in the aluminum base metal. As the friction time was increased, the joints were fractured at the interface, showing decreased tensile strength. On fracture surfaces after the tensile test, ductile areas where the tear ridge of aluminum stuck to the steel-side fracture surface decreased with an increase in friction time, and brittle areas occupied almost the whole fracture surface when the friction time was 1.5 s or more, as shown in **Figs. 14 and 15**.

TEM microstructures of the A1070/S10C joint are

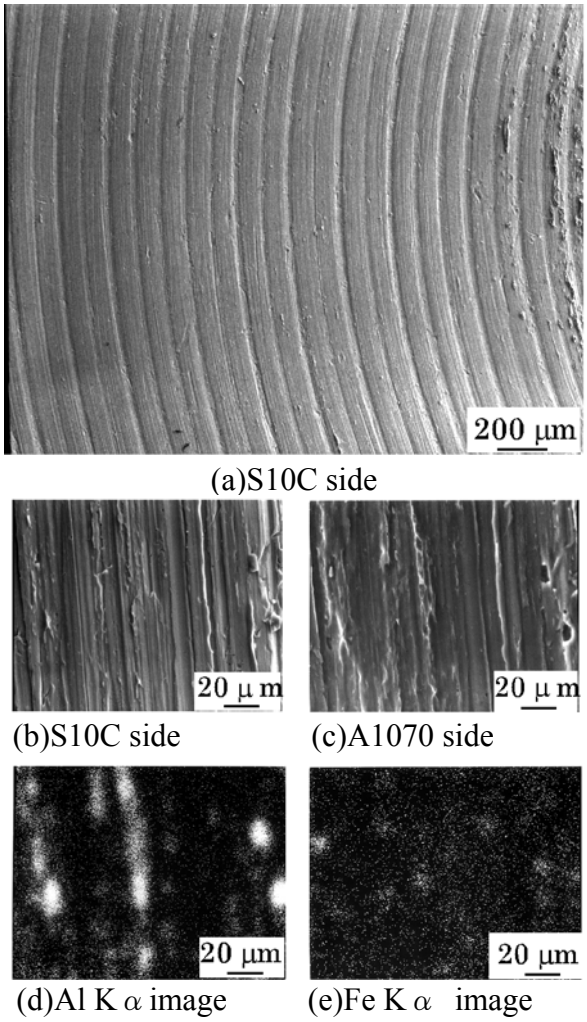

Fig. 14 Fractured surfaces of a A1070/S10C joint (t_1=1.5 s): (a) fractured surface of the steel side, (b) fractured surface of the steel side observed at a higher magnification, (c) fractured surface conjugate to (b), (d) distribution of Al analyzed by EDX in the area shown in (b), and (e) distribution of Fe analyzed by EDX in the area shown in (c).

shown in **Fig. 16**. In the joint showing the maximum tensile strength (t_1 = 0.5 s), no intermetallic compound or oxide film could be detected at the interface as shown in **Fig. 16(a)**; i.e., the aluminum and steel substrates were brought into intimate contact without an interlayer thicker than ~10 nm at the most. When the friction time was increased to 2 s, a layer of intermetallic compounds was formed at the interface as shown in **Fig. 16(b)**. The intermetallic compound was identified as Fe_2Al_5 based on SAD patterns (no other intermetallic compound could be detected). Although the layer of the intermetallic compound was no more than 100 nm thick, the fracture morphology observed in Fig. 15 suggests that this layer was responsible for the brittle fracture at the interface.

3.4 Growth of Intermetallic Compound Layer at Friction Bonded Interface [13, 15, 16, 19]

The thickness of the IMC layers observed in the A5052/S10C, A5083/S10C, and A1070/S10C joints was

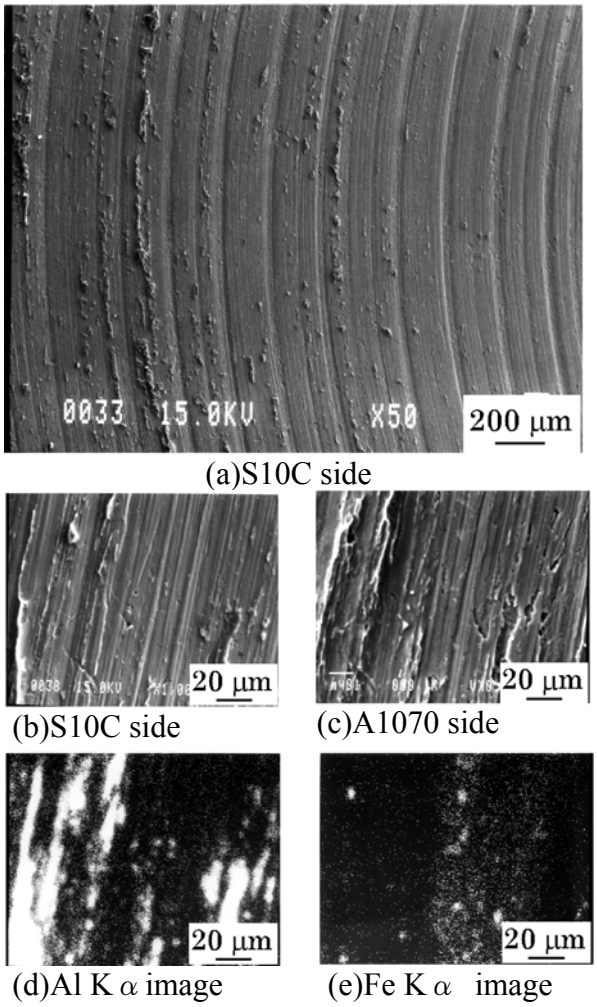

Fig. 15 Fractured surfaces of a A1070/S10C joint (t_l=2.0 s): (a) fractured surface of the steel side, (b) fractured surface of the steel side observed at a higher magnification, (c) fractured surface conjugate to (b), (d) distribution of Al analyzed by EDX in the area shown in (b), and (e) distribution of Fe analyzed by EDX in the area shown in (c).

plotted against the friction time in **Fig. 17**. Although scattered quite widely, the thickness of the IMC layers grew almost linearly with an increase in friction time for all the joints. It has been generally accepted that the thickness of the IMC layer *W*, when its growth is controlled by the diffusion of elements, increases with time, obeying a parabolic law given by [14)]

$$W = k\,t^{1/2}.$$

Therefore, the kinetics of the growth of the IMC layers shown in Fig. 17 suggests that their growth was controlled by a factor other than the diffusion. In this relation, as described in §3.1 and §3.2, morphologies and distributions of the IMCs observed in the A5052/S10C and A5083/S10C joints were different from those reported in previous papers about the IMC layer in the diffusion couple [14)]. We think that the mechanical mixing of the steel with the Al alloy contributed significantly to

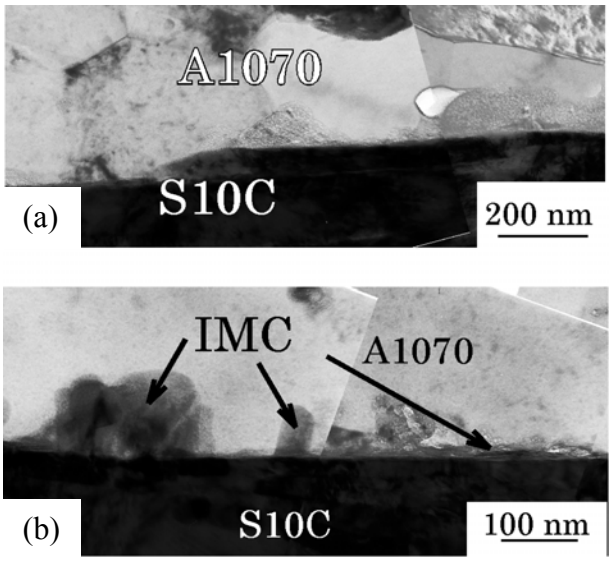

Fig. 16 TEM micrograph s of A1070/S10C joints: (a) t_l=0.5 s and (b) t_l=2 s.

the formation and growth of the IMCs for the following reasons. The grooves caused by machining with a lathe disappeared on the fractured surfaces of the steel side as the friction time was increased (see Figs. 5, 6, 9, and 10), suggesting that the steel surface was worn down during the friction process. This suggests that the incorporation of the steel into the Al alloy occurred in the friction process. It is conceivable that the very rapid and complicated plastic flow induced in the Al alloy substrate during the friction process causes mechanical mixing of the incorporated steel with the Al alloy to form the intermetallic compounds of the Al-Fe system.

3.5 Controlling Factors of Bond Strength [13, 15, 19)]

As described in §3.1 – 3.3, for all the friction-bonded joints of steel S10C to Al-alloys, A5052, A5083, and A1070, the tensile strength of the joint had a common tendency to rise to a maximum value at first, and then reduce with an increase in friction time. Observations of the fracture surfaces and interfacial microstructures suggest that the Al-oxide film of ~10 nm thickness remained at the bond interface when the tensile strength was increased with friction time, and the crack on the tensile test was developed along the oxide film. As the friction time was increased, the Al-oxide film disappeared, and in the area where no Al-oxide or intermetallic compound was detected, the crack on the tensile test was propagated through the Al alloy substrate, leaving Al-alloy tear ridges on the fracture surface. The Al-oxide film probably came from the superficial oxide film of the Al-alloy or that of the steel which reacted with Al to form the Al oxide.

When the friction time was longer than those to obtain the maximum strength, the Al oxide film at the interface was not observed, and the crack on the tensile test propagated in the IMCs layer which occupied almost the whole area of the interface. The relations between the

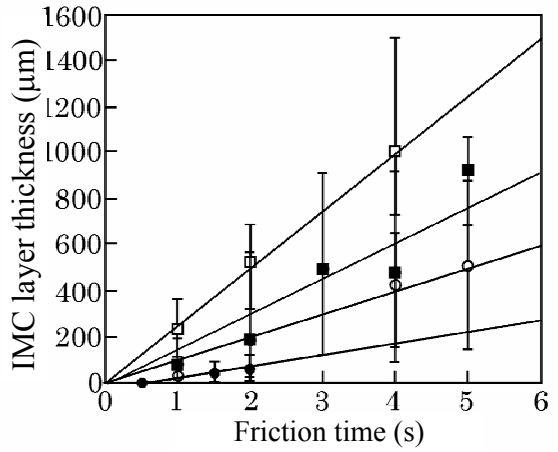

Fig. 17 Relations between the thickness of the IMCs layers and friction time for the A5052/S10C, A5083/S10C, and A1070/S10C joints(○ A5052/S10C - P_1 = 20 MPa, □ A5052/S10C - P_1 = 20 MPa, ■ A5083/S10C - P_1 = 40 MPa, ● A1070/S10C – P_1 = 20 MPa).

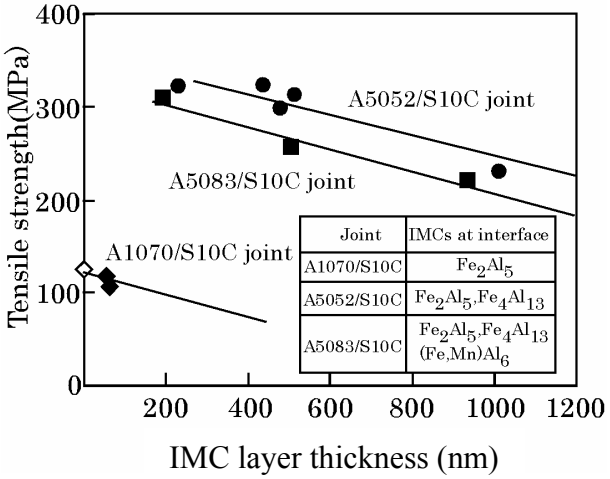

Fig. 18 Relations between the tensile strength and thickness of the IMCs layer for the A5052/S10C, A5083/S10C, and A1070/S10C joints.

tensile strength and the thickness of the IMCs layer are shown in **Fig. 18**. The tensile strength of joints which were fractured in the IMCs layer decreased with an increase in the thickness of the IMC layer for the A5052/S10C, A5083/S10C, and A1070/S10C joints. Provided that the IMCs layers were of the same thickness, the A5052/S10C joint showed tensile strength nearly equal to that of the A5083/S10C joint though the difference in those of the Al alloy base metals were quite large. For these joints, the IMC layer consisted mainly of Fe_2Al_5 and Fe_3Al_4, involving small amounts of $FeAl_2$ (in A5052/S10C joint) and (Mn, Fe)Al_6 (in A5083/S10C joint). These intermetallic compounds distributed randomly in the layer, and the crack propagated through them nonpreferentially. Thus, the tensile strength of these IMC layers can be considered to be controlled by the average properties of the involved intermetallic compounds. Since the IMC layers of the A5052/S10C and A5083/S10C joints consisted mainly of Fe_2Al_5 and Fe_4Al_{13}, these joints were fractured at almost the same stresses when the IMC layers were the same thickness. In other words, the tensile strength of these joints was controlled by the mechanical properties of the IMCs layer.

When the friction time was 4 s, viz., when the $MgAl_2O_4$ layer was formed in addition to the intermetallic compounds, the 5083/S10C joint showed much lower tensile strength than that estimated from the IMC layer thickness using the relation shown in Fig. 18. This result suggests that the $MgAl_2O_4$ layer impaired the joint strength more seriously than the IMC layer.

The tensile strength of the A1070/S10C joint was much lower than those of the A5052/S10C and A5083/S10C joints having the IMCs layers of the same thickness. The reason for this cannot be explained well. As described in §3.3, however, the IMC layer of A1070/S10C joint consisted of only Fe_2Al_5 in contrast to those of the A5052/S10C and 5083/S10C joints which involved $FeAl_2$, Fe_2Al_5, Fe_4Al_{13}, and (Mn,Fe)Al_6. It has been reported that the tensile strength of Fe_2Al_5 is much poorer than Fe_4Al_{13} [9]. As mentioned above (§3.5), the crack on the tensile test propagated through grains of Fe_2Al_5, Fe_4Al_{13}, $FeAl_2$ (A5052/S10C joint), and (Mn, Fe)Al_6 (A5083/S10C joint) nonpreferentially. The compounds other than Fe_2Al_5 can be considered to obstruct the crack propagation compared with Fe_2Al_5. Probably, this effect of the compounds other than Fe_2Al_5 will contribute to the higher tensile strength of the A5052/S10C and A5083/S10C joints than that of the A1070/S10C

4. Conclusions

The nano-scale microstructures of the friction-bonded interfaces of low carbon steel S10C to Al alloys 5052, 5083, and A1070 have been investigated mainly by TEM observation to discuss the controlling factor of bond strength of the interface. Results obtained can be summarized as follows:

(1) The intermetallic compounds were formed in the interfacial layer less than 1 μm in thickness even when they were undetectable with a light microscope. The intermetallic compounds observed were $FeAl_2$, Fe_2Al_5, and Fe_4Al_{13} for the A5052/S10C joint, Fe_2Al_5, Fe_4Al_{13}, (Mn,Fe)Al_6 and Mg_2Si for the A5083/S10C joint, and Fe_2Al_5 for the A1070/S10C joint. At the interface of A5083/S10C joint, $MgAl_2O_4$ was also formed in addition to the intermetallic compounds. The formation of these compounds at the interface suggests a strong influence of alloying elements on the formed intermetallic compound. The intermetallic compounds were granular, distributed randomly in the interfacial layer, and the thickness of the layer increased almost linearly with friction time, suggesting that their formation and growth were controlled by a factor other than the diffusion of elements. An Al-oxide film was also observed at the interface for all the joints prior to the substantial

formation of the intermetallic compounds. With an increase in friction time, the Al oxide film was disappeared.

(2) The strength of the joint interface increased with friction time at first, and then decreased after reaching a maximum level at friction times depending on the Al alloy.

(3) The microstructures controlling the joint strength can be considered to be the Al oxide film when the friction time was less than that to obtain the maximum strength, and the IMCs layer when the friction time exceeded that to obtain the maximum strength. The $MgAl_2O_4$ layer is thought to have even worse influence on the bond strength than the layer of the intermetallic compounds.

References

1) F. Matsuda: Welding Technology, No.11(1974), 15 (in Japanese).
2) J. Seretsky and E.R. Ryba: Weld. J., 55(1976), 208-s.
3) G. Metzger and R. Lison: Weld. J., 55(1976), 230-s.
4) S. Katayama: Welding Technology, 50-2(2002), 69 (in Japanese).
5) H. Oikawa, T. Saito, T. Yoshimura, T. Nagase, and T. Kiriyama: Quarter. J. JWS., 14-2(1996), 267 (in Japanese).
6) R.F. Tylecote: Brit. Weld. J., 1(1954), 117.
7) S. Elliott and E.R. Wallach: Metal Construction, (1981), 167.
8) S. Elliott and E.R. Wallach: Metal Construction, (1981), 221.
9) S. Mukae, K. Nishio, M. Katoh, T. Inoue and K. Sumitomo: Quarter. J. JWS, 12(1994), 528 (in Japanese).
10) H. Oikawa, T. Saito, T. Yoshimura, T. Nagase, and T. Kiriyama: Tetsu-to-hagane, 83(1997), 641 (in Japanese).
11) G. Kawai, K Ogawa, H.Ochi, and H. Tokisue: J. Light Metal & Const., 37(1999), 295 (in Japanese).
12) T. Shinoda, M. Ogawa, S. Endo, and K. Miyahara: Quarter. J. JWS, 18(2000), 365 (in Japanese).
13) N. Yamamoto, M. Takahashi, M. Aritoshi and K. Ikeuchi: Quarter. J. JWS, 23 (2005), 352 (in Japanese).
14) K.Shibata, S. Morozumi and S. Koda: J. Japan Institute of Metals, 30 (1966), 382 (in Japanese).
15) N. Yamamoto, M. Takahashi, M. Aritoshi and K. Ikeuchi: Quarter. J. JWS, 23(2005), to be published (in Japanese).
16) N. Yamamoto, M. Takahashi, K. Ikeuchi and M. Aritoshi: Mater. Trans. JIM, 2(2004), 296.
17) G. Petzow and G. Effenberg: *Ternary Alloys Vol. 5*, VCH Publishers, New York, (1992), 250.
18) A. Hasui and S. Fukushima: J. Japan Weld. Soc., 44(1975), 1005 (in Japanese).
19) N. Yamamoto, M. Takahashi, M. Aritoshi and K. Ikeuchi: Quarter. J. JWS, submitted (in Japanese).